Physical Properties of Fullerene-containing Galactic Planetary Nebulae

M. Otsuka[*,1]**, F. Kemper**[1]**, J. Cami**[2,3]**, E. Peeters**[2,3]**, J. Bernard-Salas**[4]

[1]*Institute of Astronomy and Astrophysics, Academia Sinica, 11F of Astronomy-Mathematics Building, AS/NTU. No.1, Sec. 4, Roosevelt Rd, Taipei 10617, Taiwan, R.O.C.*
[2]*Department of Physics and Astronomy, The University of Western Ontario, London, ON N6A 3K7, Canada*
[3]*SETI Institute, 189 Bernardo Ave, Suite 100, Mountain View, CA 94043, USA*
[4]*Department of Physical Sciences, The Open University, Milton Keynes, MK7 6AA, UK*
E-mail: `otsuka@asiaa.sinica.edu.tw`

We searched the *Spitzer* Space Telescope data archive for Galactic planetary nebulae (PNe), that show the characteristic 17.4 and 18.9 μm features due to C_{60}, also known as buckminsterfullerene. Out of 338 objects with *Spitzer*/IRS data, we found eleven C_{60}-containing PNe, six of which (Hen2-68, IC2501, K3-62, M1-6, M1-9, and SaSt2-3) are new detections. The strongest 17.4 and 18.9 μm C_{60} features are seen in Tc 1 and SaSt 2-3, and these two sources also prominently show the C_{60} resonances at 7.0 and 8.5 μm. In the other nine sources, the 7.0 and 8.5 μm features due to C_{60} are much weaker. The flux ratio between the 17.4 and 18.9 μm C_{60} feature is rather constant amongst the sample, with an average value of 0.49. We find that the Polycyclic Aromatic Hydrocarbon (PAH) profile over 6-9 μm in these C_{60}-bearing carbon-rich PNe is of the more chemically-processed class A. The *Spitzer* spectra also show broad dust features around 11 and 30 μm. The strength of the 11-μm feature is correlated to the temperature of the dust, suggesting that it is at least partially due to a solid-state carrier.

The Life Cycle of Dust in the Universe: Observations, Theory, and Laboratory Experiments
18-22 November, 2013
Taipei, Taiwan

---

[*]Speaker.
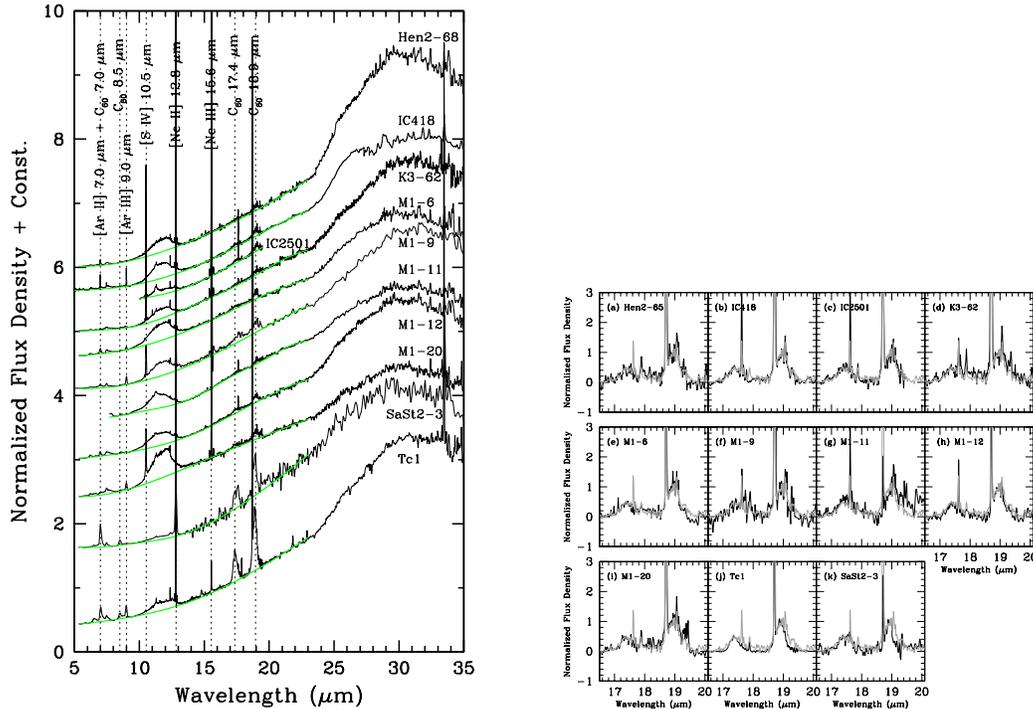
Figure 1: (*left*) The 5.3-35 μm *Spitzer*/IRS and *ISO* spectra normalized to the flux density at 20 μm. The green lines are base lines determined by fitting the underlying feature-less continuum with third to fifth order spline in the range from 5.3 to 23 μm, except for IC2501 and M1-11. For IC2501 we determined the continuum over 2.5-5.0 μm and 10-19.6 μm, while for M1-11 we used 2.5-5.0 and 8-23 μm. The flux density normalization for IC2501 was using the extrapolated continuum from 10-19.6 μm continuum (the green line). (*right*) The local continuum subtracted spectra over 16.5-20.1 μm, normalized to the peak flux density in the 18.9 μm C_{60} band. The black lines represent the observed spectra of each object and the grey lines show the average spectrum among all objects.

1. Results

We summarize our analyses of the *Spitzer*/IRS and *ISO*/SWS mid-infrared spectra of C_{60} PNe as follows. The detailed discussion is found in Otsuka et al. (2014) [1]. The broad 30 μm feature in our sample is discussed by Kemper et al. [2] in these proceedings.

Spectral Features and Variations in 5-36 μm　　The 5.3-35 μm spectra are presented in Figure 1 left. There are strong variations in the intensity of the 8.5, 17.4, and 18.9 μm C_{60} bands relative to the local dust continuum indicated by the green lines, with SaSt2-3 and Tc1 showing especially strong 8.5, 17.4, and 18.9 μm C_{60} bands. The 6-9 μm PAH bands are seen in all PNe, although the band-profiles are different from ones frequently seen in non-C_{60} PNe. The broad 11 and 30 μm features are also seen in all PNe. All the spectra show a thermal dust continuum. Otsuka et al. (2014) [1] show that the dust continuum slope is different for the different objects, pointing to different dust temperatures, caused by the difference in irradiation (see their Figure 3). They found that the strengths of the 17.4 μm and 18.9 μm C_{60} bands are not changing with the local dust continuum.
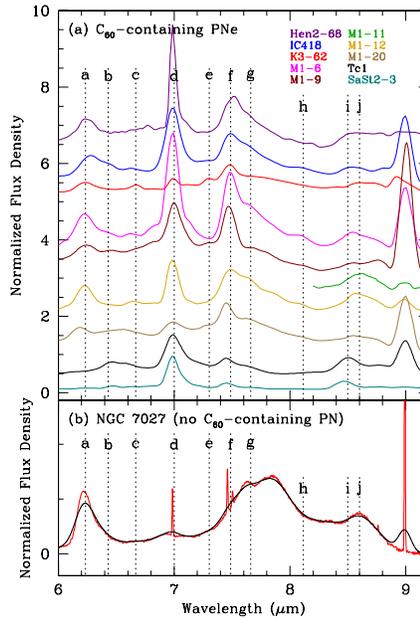
Figure 2: (*upper panel*) The continuum subtracted over 6.0-9.2 μm PAH line-profiles of C_{60} PNe. (*lower panel*) The *ISO*/SWS spectrum of the C-rich PN NGC7027. The high-excitation gas lines are subtracted out. The resolution of this spectrum (red line) was reduced to that of *Spitzer*/IRS (black line). The emission features seen in these spectra are indicated by dotted lines and lower-case letters. a: PAH C=C stretch 6.23 μm, b: C_{60}^+ 6.4 μm (possible), c: C_{24} planar (possible) or PAH C=C stretch 6.67 μm, d: C_{60} 7.0 μm + [Ar II] 6.99 μm, e: an emission feature at 7.30 μm seen by Scott & Duley (1996) [3] and Scott et al. (1997) [4], f: C_{60}^+ + H I complex, g: PAH C-C stretch 7.7 μm, h: C_{60}^+ 8.1 μm (possible), i: C_{60} 8.5 μm, j: PAH C-H in-plane bend 8.6 μm.

The 17.4 and 18.9 μm C_{60} line profiles   Figure 1 right displays the continuum subtracted spectra (black lines), showing the 17.4 and 18.9 μm C_{60} bands. The normalized line profiles of the 17.4 and 18.9 μm C_{60} bands are similar to each other, as can be seen from the average spectrum (grey line). The flux ratio between the 17.4 and 18.9 μm C_{60} feature is rather constant amongst the sample, with an average value of 0.49.

The 7.0 and 8.5 μm C_{60} and the broad 6-9 μm complex   The line-profiles are similar to each other, except for the 6.2 and 8.5 μm bands (Figure 2). There is the possibility that the 6.99 and 7.07 μm C_{70} resonances might contribute to the 7.0 μm band. However, we could not detect any C_{70} bands in our sample, except for the already reported features in Tc1 (Cami et al. 2010 [5]). Therefore, in the PNe in our sample except for Tc1, the 7.0 μm line is concluded to be due to a complex of the 6.92 μm aliphatic vibration band, the [Ar II] 6.99 μm, and the 7.0 μm C_{60} band. Tc1 and SaSt2-3 clearly show the strong 8.5 μm C_{60} band, while the 6.2 μm PAH band is very weak. In other sources these bands are heavily contaminated by PAHs at 8.6 and 6.2 μm, respectively. The 7.2-8.1 μm band profiles are quite different from that in a Class B PAH C-rich PN NGC7027. Class B PAH objects exhibit the emission peak at $\sim$7.8-8 μm (Peeters et al. 2002 [6]), while C_{60} PNe emit the bulk of their emission around $\sim$7.7 μm. Hence, according to the classification of the 6-9 μm PAH profiles, all C_{60} PNe exhibit Class A PAH profiles. The carrier of
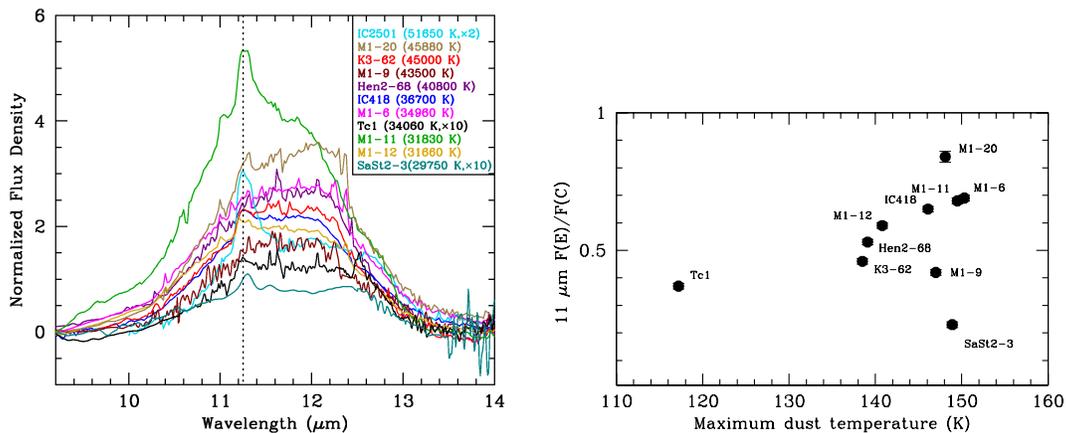
Figure 3: (*left*) The continuum subtracted spectra over 9.1-14 μm, normalized to the peak flux density of C_{60} 18.9 μm, except for IC2501, SaSt2-3, and Tc1. The scaling factor for these PNe are 2, 10, and 10 after the normalization to C_{60} 18.9 μm. The effective temperatures of the PN central stars are listed in the upper-right corner. The position of the 11.3 μm PAH is indicated by the dotted line. (*right*) The plot between the band strength of the broad 11 μm band and the maximum dust temperature.

the Class A is believed to be more chemically processed than that of the Class B profiles.

The broad 11 μm feature   The emission profiles show a nearly flat portion between 11.2 and 12.4 μm, except for M1-11 (Figure 3 left). The peak intensity of the 11 μm feature in SaSt2-3 and Tc1, which show the prominent C_{60} bands, is much weaker than in the other PNe. A correlation between the 11 μm band strength and the maximum dust temperature, suggests that the carrier of this feature is a thermally heated dust component (Figure 3 right). On the other hand, the substructure in the 11 μm feature points to a carrier related to PAHs. Kwok et al. (2001) [7] argue that the 11 μm feature is a collection of out-of-plane bending modes of aliphatic side groups attached to aromatic rings. Further discussion about the carrier is necessary.

References

[1] M. Otsuka et al. 2014 *Physical properties of fullerene-containing Galactic planetary nebulae*, *MNRAS*, **437**, 2577

[2] F. Kemper et al, *On the nature of the 30 micron feature in carbon-rich planetary nebula* , in proceedings of *The Life Cycle of Dust in the Universe: Observations, Theory, and Laboratory Experiments*, PoS(LCDU2013)122.

[3] A. Scott and W. W. Duley 1996 *The Decomposition of Hydrogenated Amorphous Carbon: A Connection with Polycyclic Aromatic Hydrocarbon Molecules*, *ApJL*, **472**, L123

[4] A. D. Scott et al. 1997 *Infrared Emission Spectra from Hydrogenated Amorphous Carbon*, *ApJL*, **490**, L175

[5] J. Cami et al. 2010 *Detection of C_{60} and C_{70} in a Young Planetary Nebula*, *Science*, **329**, 1180

[6] E. Peeters et al. 2002 *The rich 6 to 9 μm spectrum of interstellar PAHs*, *A&A*, **390**, 1089

[7] S. Kwok et al. *On the Origin of Infrared Plateau Features in Proto-Planetary Nebulae*, *ApJL*, **554**, L87